Δελτίο της Ελληνικής Γεωλογικής Εταιρίας, 2010
Πρακτικά 12ου Διεθνούς Συνεδρίου
Πάτρα, Μάιος 2010

Bulletin of the Geological Society of Greece, 2010
Proceedings of the 12th International Congress
Patras, May, 2010

SEISMICITY CHANGES DETECTION DURING THE SEISMIC SEQUENCES EVOLUTION AS EVIDENCE OF STRESS CHANGES

Astiopoulos A. C.[1], Papadimitriou E.[1], Karakostas V[1], Gospodinov D. [2], and Drakatos G.[3]

[1] *Geophysics Department, School of Geology, Aristotle University of Thessaloniki, GR54124 Thessaloniki, tasosast@geo.auth.gr, ritsa@geo.auth.gr, vkarak@geo.auth.gr*

[2] *Geophysical Institute, Bulgarian Academy of Sciences, Sofia, Bulgaria, drago_pld@yahoo.com*

[3] *Institute of Geodynamics, National Observatory of Athens, GR11810, g.drakat@gein.noa.gr*

Abstract

The statistical properties of the aftershock occurrence are among the main issues in investigating the earthquake generation process. Seismicity rate changes during a seismic sequence, which are detected by the application of statistical models, are proved to be precursors of strong events occurring during the seismic excitation. Application of these models provides a tool in assessing the imminent seismic hazard, oftentimes by the estimation of the expected occurrence rate and comparison of the predicted rate with the observed one. The aim of this study is to examine the temporal distribution and especially the occurrence rate variations of aftershocks for two seismic sequences that took place, the first one near Skyros island in 2001 and the second one near Lefkada island in 2003, in order to detect and determine rate changes in connection with the evolution of the seismic activity. Analysis is performed through space–time stochastic models which are developed, based upon both aftershocks clustering studies and specific assumptions. The models applied are the Modified Omori Formula (MOF), the Epidemic Type Aftershock Sequence (ETAS) and the Restricted Epidemic Type Aftershock Sequence (RETAS). The modelling of seismicity rate changes, during the evolution of the particular seismic sequences, is then attempted in association with and as evidence of static stress changes.

Key words: *aftershock sequence, stochastic models, seismic quiescence, MOF, ETAS, RETAS, Coulomb stress changes.*

1. Introduction

Seismicity anomalies during the seismic sequences evolution and especially the seismic quiescence phenomenon have attracted much attention as one of the precursors to a large earthquake (Utsu, 1968; Ohtake et al., 1997; Wyss and Burford, 1987; Kislinger, 1988; Ogata, 1992, 1999). Its recognition in complex aftershock sequences, where the activity is high, is difficult. Nowadays, the application of statistical models has prevailed, in order to point out such a phenomenon. Interpreting the model application results in association with the corresponding results of other processes such as the Coulomb stress changes due to the coseismic slip of strong main shocks, can provide a tool in assessing the imminent seismic hazard.

Aiming to reveal the evolution pattern of two seismic sequences that took place in the Greek territory, the first one in the vicinity of Skyros Island, in 2001, and the second one along the west coast of Lefkada Island, in 2003, the aftershocks' temporal behaviour is examined based upon the application of Gospodinov and Rotondi (2006) software. This includes the selection of the appropriate statistical model, among MOF (Utsu, 1969), ETAS (Ogata, 1988) and RETAS (Gospodinov and Rotondi, 2006) and the data elaboration based upon the selected model. The spatial distribution of the static stress changes that resulted from the main shocks, are associated either with relative quiescence or excitation of the aftershock activity, which is observed when examining the aftershocks temporal distribution.

2. Method

2.1 Statistical models

The first statistical approach for the temporal distribution of aftershocks was introduced by Omori (1894), the well known Omori Law, which relates the aftershock occurrence rate, $\lambda(t)$, gradual decay in a time interval, t, after the main shock occurrence, with the relation:

(1)

where c and K are parameters. Relation (1) was transformed by Utsu (1969), in the Modified Omori Formula (MOF):

(2)

where p is a parameter indicative for a seismic sequence, expressing regional properties.

Ogata (1988) proposed the idea of self – similarity by extending the capacity of generating secondary events to every aftershock of the sequence through the formulation of the Epidemic Type Aftershock Sequence (ETAS) whose conditional intensity function is:

(3)

where every i corresponds to every event at time t_i.

Gospodinov and Rotondi (2006) offer the Restricted Epidemic Type Aftershock Sequence (RETAS) model, which is based on the assumption that not all events in a sample but only aftershocks with magnitudes larger than or equal to a threshold M_{th} can induce secondary seismicity. Then the conditional intensity function for the model is formulated as:

(4)

Varying M_{th} between the cut–off magnitude M_o and the main shock magnitude M_i, different versions of RETAS are examined, between ETAS and MOF models, considering these two models as limit cases.

2.2 Parameters estimation

For the models parameters Ogata (1983) proposed the maximum likelihood estimates (MLE) which maximize the log–likelihood function. A single form for this function is (Gospodinov and Rotondi, 2006):

(5)

where N is the number of earthquakes of magnitude larger than or equal to M_o which occur at times t_i, i = 1,...,N, in the interval under study [0, T].

2.3 Akaike criterion

A large number of statistical models can be applied at every seismic sequence. Thus, the Akaike Information Criterion (AIC, Akaike, 1974) is used as a measure for selecting the best among competing models for a fixed data set. It is defined by:

(6)

where θ stands for the model parameters, L is the maximum likelihood for a particular model, and k is the number of parameters of the model. The model with the smaller AIC shows the better fit to the data.

2.4 Residual process analysis

Having obtained the best among the proposed models (Akaike criterion), there is still the possibility of the existence of a better one. It can be seen precisely how well or poorly the estimated model is fitted to an aftershock sequence by inspecting the cumulative number of aftershocks with respect to the transformed time (Ogata, 1988). The integration of the nonnegative conditional intensity function produces a transformation of time from t to τ so that the occurrence time t_j are transformed 1:1 into τ_j and the earthquakes follow the standard stationary Poisson process on the new axis if the intensity function is the true one for the data:

(7)

The process is called a **residual process** and its mean and standard deviation are used to study possible deviations of the data from the model (Ogata, 1992).

2.5 Coulomb stress changes calculations

This process includes the static stress changes calculations and the examination of their spatial distribution in connection with the spatial distribution of the aftershock activity. It has been observed in several cases that in addition to the main rupture, neighboring fault segments or minor active structures are activated soon after the main occurrence, which are the sources of aftershock clustering both in space and time. Oftentimes, relative quiescence takes place before this secondary activation. These occurrence patterns in the aftershock activity are then interpreted in terms of the stress field static changes.

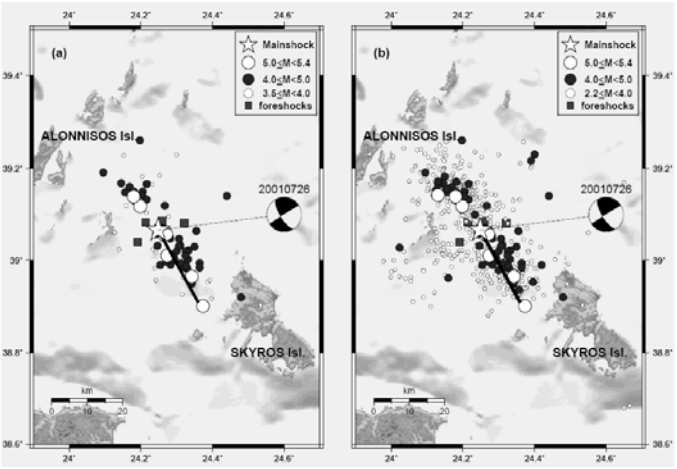

Fig. 1: a) The spatial distribution of the aftershocks ($M_w \geq 3.5$) which occurred in the first day after the main shock. Two separate clusters are shown, the one associated with the main rupture (black continuous line) and the second with an along strike adjacent fault segment. b) Spatial distribution of the aftershocks ($M_w \geq 2.2$) which occurred in the first month after the main shock. In addition to the activated segments shown in (a), a third cluster appears which striking NE–SW.

2.6 Data

The data used for the current analysis are taken from the monthly bulletins of the Central Seismological Station of Geophysics Department of the Aristotle University of Thessaloniki and the Institute of Geodynamics of the National Observatory of Athens. A unified catalog was compiled which covers the time interval from the beginning of each seismic sequence up to February of 2009. The data samples were checked for completeness and a threshold magnitude was assigned for each seismic sequence.

3. Seismic sequences analysis

3.1 Skyros seismic sequence

On 26 July 2001 an earthquake of $M_w = 6.4$ occurred at the submarine area between the islands of Allonisos and Skyros (39.05°N, 24.248°E), at the western part of central Aegean Sea. The rupture took place on a left–lateral NW–SE trending strike slip fault with a length of about 24 km (Karakostas et al., 2003). North Aegean region is dominated by right–lateral strike slip faults, trending NE-SW, as well as smaller normal faults (Papazachos et al., 1998). The fault which is connected with the main shock is conjugate to the right–lateral ones and appears to mark the boundary between them and the E–W trending normal faults of the Greek mainland (Karakostas et al., 2003). The sequence was attracted the interest of several scientists resulted in source models and stress field analysis (Zahradnik, 2002; Roumelioti et al., 2004; Ganas et al., 2005).

Aftershock activity was particularly intense, with seven aftershocks of $M_w \geq 5.0$ in the first day after the main shock occurrence. The epicentral distribution of the aftershocks of $M_w \geq 3.5$ which occurred in the first day delineate the main rupture, along with an along strike activated neighboring fault segment (Karakostas et al., 2003; Figure 1a). Smaller magnitude ($M_w \geq 2.2$) aftershock activity continued for a month onto the aforementioned segments, along with onto a seismic band to the WSW from the main shock epicenter, striking NE–SW (Figure 1b).

The RETAS model was applied on two data sets. Firstly, a catalogue of aftershocks was considered that covers the period from 26 July 2001 up to 26 February 2009, in a zone defined by the vertices 38.6°N–23.9°E; 39.3°N–24.8°E. The magnitude of completeness, calculated by the ZMAP software package (Wiemer and Zuniga, 2001) was found equal to M_o=3.5, which resulted to 449 events re-

Table 1. Model parameters estimated for two data sets, for Skyros sequence, 2001.

Data sets	Model	M_{th}	AIC	μ	k	α	c	p
26/07/2001–26/02/2009	ETAS	3.5	437.553	0	0.032	1.803	0.029	1.046
26/07/2001–30/07/2001	RETAS	4.0	-679.516	0	0.123	0.971	0.003	0.896

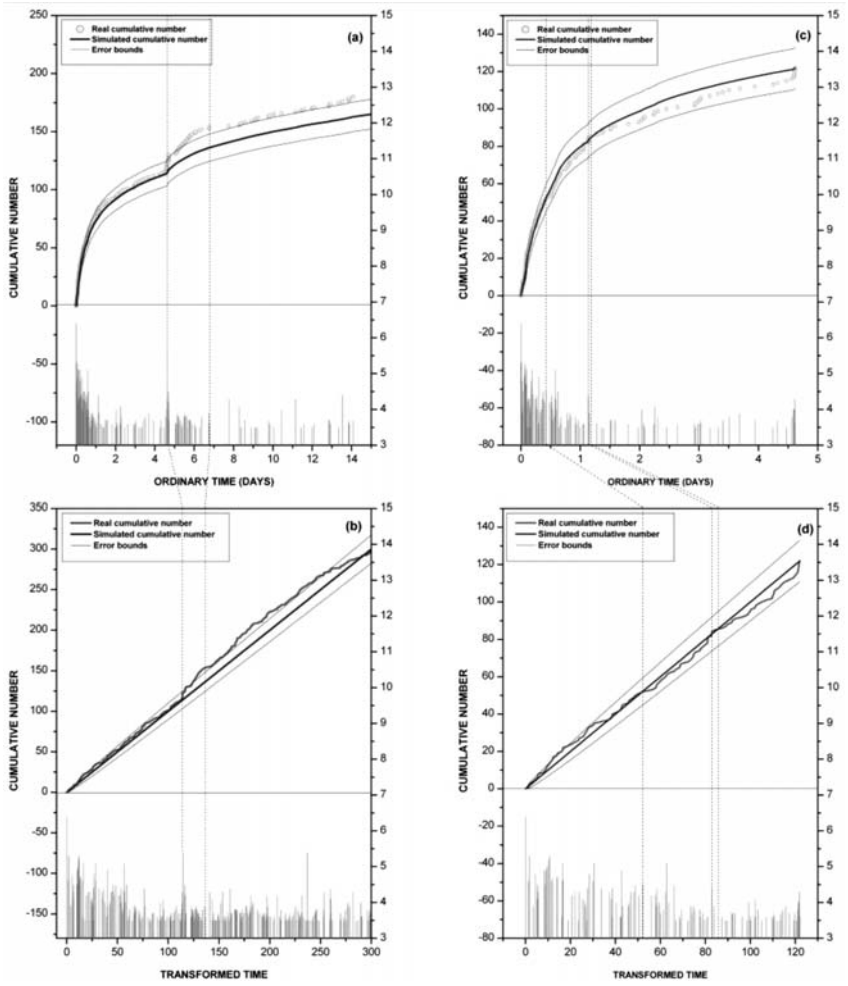

Fig. 2: Cumulative number of earthquakes (yellow circles and red solid lines) against ordinary (a, c) and transformed (b, d) lapse time respectively, in addition to the theoretically expected cumulative function (blue solid lines) due to the best fitting statistical model. Thin, solid blue lines stand for error bounds. Dashed lines appoint specific time periods and moments during the sequence evolution.

maining in the complete catalogue. The smallest AIC value as it is calculated by the Akaike criterion corresponds to the magnitude M_{th}=3.5 which is the smallest of the particular data set. Subsequently, ETAS is the best model to fit the data, meaning that all events with $M_o \geq 3.5$ are capable to produce secondary aftershocks. The estimated model parameters, for two data sets, μ, for the back-

ground seismicity, k which is related to the of the main shock and the cut-off magnitude M_o, α which measures the magnitude efficiency of a shock in generating its aftershock activity, c which is a regularizing time scale that ensures that the seismicity rate remains finite close to the main shock and p that is a coefficient of attenuation are shown in Table1. The table also contains the best fitting model, the smallest AIC value and the corresponding magnitude, M_{th}.

The model fitness to the data is verified graphically through the cumulative number curves. Real and expected number of aftershocks are plotted versus the normal and transformed time (Fig. 2). Yellow circles and solid red line indicate the real cumulative number of aftershocks and solid blue line represents the expected cumulative number curve. Figures 2a and 2c show the process in real time whereas Figures 2b and 2d depict the process in transformed time. Thin solid blue lines stand for error bounds determined after the standard deviation of the model process. Figures 2a and 2b show the curves for a 15–days period after the main shock occurrence. Generally, a quite good fit of the expected to real data for the whole period is revealed, except for a two days interval (between the dashed lines) immediately after the main shock, when an M_w=5.4 aftershock occurred on 30 July 2001. Obviously, the seismic activity increased after this event (first dashed line). Unlikely, relative seismic quiescence precursor to this large aftershock was not appeared. Particularly, in Figure 2b it is recognized that the activation period is separated in two sub-periods (red curve's slope). The first sub-period lasts two hours and the occurrence rate is highly increased, while the second one lasts about 44 hours and the occurrence rate seems to be decreased.

The above process was based on a 7.5 years data set and revealed seismicity behaviour, taking into account the whole data set. In order to identify possible deviations in real time before the M5.4 aftershock occurrence, the RETAS model is applied on a second data set which contains events that belong to the same zone, as defined previously, but they occurred in the time interval from the main shock up just before this aftershock (up to 30/07/2001). The magnitude threshold was found equal to M_o=3.5, above which the data were assessed to be complete, with the final number of events for processing to be equal to 123. The smallest AIC was calculated for M_{th}=4.0, which identifies that the best fit model is RETAS with the corresponding triggering magnitude. Model's parameters are shown in table 1.

In Figures 2c and 2d a period of relative quiescence is revealed before the large aftershock occurrence, which was not evidenced previously in Figures 2a and 2b, when the larger data set was considered. This means that the aftershocks which occurred after this particular aftershock affected and changed the temporal distribution of the events that occurred before. Relative quiescence begins about 10 hours after the main shock (first dashed line), it is interrupted for a time interval of about 20 minutes (between second and third dashed line), because of a cluster of aftershocks that occurred 17 hours after the beginning of the quiescence period, and reaches the large aftershock about 3 days later, with a total duration of about 4 days.

In order to investigate the possible triggering of this secondary sequence, in other words the "sequence in a sequence", the spatial distribution of its members are superimposed on the spatial distribution of the static stress changes due to the main shock co seismic slip. For this reason the stress field changes are calculated for an observational plane parallel to the aftershock zone which trends NW of the main shock (140°/70°/-110°), at a depth of 12 km and an apparent coefficient of friction μ'=0.6. Figure 3a shows the spatial distribution of Coulomb stress changes along with the epicenters of aftershocks that occurred during the first sub-period that corresponds to the particularly increased seismicity. It is observed that the aftershocks of the first sub-period and the largest aftershock epicenters are located into the northern lobe of the positive stress changes. The spatial distribution

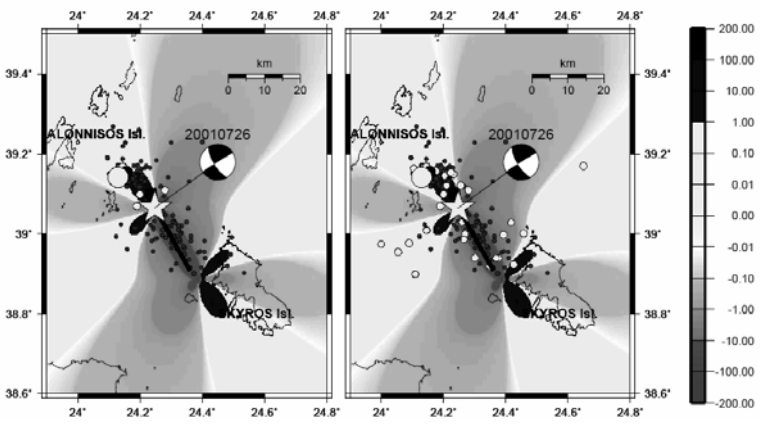

Fig. 3: Coulomb stress changes (in bars), due to Skyros main shock, calculated at a depth of 12 km, with $\mu'=0.6$, for an observational plane parallel to the aftershock zone which trends NW of the main shock epicenter (140°/70°/-110°). The distribution of aftershock epicenters are shown for (a) the first sub-period and (b) for the whole period. Main shock is depicted by a yellow star, the M5.4 aftershock with a green circle, aftershocks of magnitudes $4.0 \leq M_w \leq 5.0$ with red circles, aftershocks of magnitudes $3.5 \leq M_w < 4.0$ with yellow circles and the aftershocks prior to the M5.4 with blue circles.

of all aftershocks are plotted onto the stress field static changes in Figure 3b, where in addition to the clustered activity inside the northern lobe, a cluster is observed inside the southwestern lobe of positive stress changes. The precursory relative quiescence in association with the location of the lobes of positive static stress changes, explain satisfactorily the time and location of the largest aftershock occurrence.

3.2 Lefkada seismic sequence

On 14 August 2003 an earthquake of magnitude $M_w=6.2$ occurred near the NW coast of Lefkada Island (38.744°N–20.539°E). It is associated with a dextral strike slip fault, trending NNE–SSW with a length of about 15 km (Karakostas et al., 2004). This fault is a part of Lefkada segment of the Cephalonia Transform Fault Zone (CTFZ, Scordilis et al., 1985). Lefkada and Cephalonia constitute the most active regions, in terms of shallow seismicity, in the broader Aegean region. The CTFZ is considered to be the boundary between the continental collision of the Outer Hellenides and the Adriatic micro plate to the north and the oceanic subduction of the Eastern Mediterranean lithosphere under the Aegean Sea to the south (Papazachos and Comninakis, 1971).

Intense aftershock activity followed the occurrence of the main shock. The main cluster of aftershocks is located to the NW of the island, defining a NNE–SSW seismic band, in agreement with the strike of one of the main shock nodal planes (18°/60°/–175°), which is considered the fault plane (Karakostas et al., 2004). Main shock epicenter is located at the southern part of this cluster, implying a unilateral rupture, whereas two more clusters, well separated, appeared to the north and south of the main cluster, respectively (Karakostas, 2008). Aftershock activity also extended from the SW edge of Lefkada Island up to the NW coasts of Cephalonia Island, probably triggered by the main shock since it was located inside a lobe of positive static stress changes (Karakostas et al., 2004).

The RETAS model applied onto three data sets. The events of the first data set occurred during the

Table 2. Model parameters estimated for three data sets, for Lefkada sequence, 2001

Data sets	Model	M_{th}	AIC	μ	k	α	c	p
14/08/2003-01/02/2009	ETAS	3.8	623.943	0	0.025	2.68	0.094	1.059
14/08/2003-16/11/2003	MOF	6.2	-365.929	0	17.741	1.106	2.585	1.691
14/08/2003-25/03/2007	ETAS	3.7	283.41	0	0.026	2.767	0.228	1.092

period 14 August 2003–1 February 2009 in a region defined by the vertices 38.2°–20.1°, 39.1°–20.8°. A completeness magnitude of M_o=3.8 was estimated by the ZMAP software and thus a complete catalogue of 464 aftershocks was derived. The smallest AIC value was calculated for M_{th}=3.8 which implies that the best–fit model is ETAS and thus, each aftershock of M≥3.8 can trigger secondary aftershocks. Model's parameters are shown in Table 2.

Two periods of intense activation which followed the occurrence of the main shock and of a M5.7 event, respectively, are shown in Figure 4a. The later, occurred on 25 March 2007 near the NW Coast of Cephalonia Island (second dashed line), which is comprised into the study area. A smaller activation was triggered by an aftershock of magnitude M_w=4.8 which occurred on 16 November 2003 (first dash line). Model's fitting at the intense activation which follows the main shock (Fig. 4b) is insufficient. Periods of relative seismic quiescence which are connected with the large aftershocks are also revealed (Fig. 4b). The above process was based on the first data set which includes the aftershocks that occurred during the whole time interval from 2001 up to 2009. In order to seek for possible quiescence periods precursor to the aforementioned M4.8 and M5.7 events, in real time, the RETAS model is applied on two different data sets with events that occurred at the same region, as defined previously, but in more confined time intervals, that is from the main shock up just before the occurrence times of these two shocks, respectively.

Thus, in the case of the M4.8 event, a catalogue of 175 events was considered, with a magnitude cut-off of M_w=3.8, determined with the ZMAP software (Wiemer and Zuniga, 2001). The smallest AIC value is for a triggering magnitude of M_{th}=6.2, which is equal to the magnitude of the main shock and this result recognizes the MOF model to fit best the aftershock temporal evolution of this particular data set. This means that only the main shock can trigger secondary aftershocks. Model parameters are shown in table 2. Figures 4c and 4d evidence that the model fits very well the data, while a period of relative seismic quiescence prior to the M4.8 event is not observed.

In the case of the M5.7 event, a catalogue of 397 aftershocks was prepared, with magnitudes above the cut–off M_o=3.7 determined by the ZMAP software. The smallest AIC was calculated for M_{th}=3.7 which identifies the best fit model to be ETAS. Model's parameters are shown in table 2. Figures 4e and 4f show that this particular model cannot fit sufficiently well the temporal evolution pattern of the real data, because periods are revealed in which the curve of the expected, by the model, data exceeds the error bounds.

In order to investigate the possible triggering of the sequences which followed with main shocks of M4.8 (16/11/2003) (secondary sequence) and M5.7 (25/03/2007), the aftershock spatial distributions are plotted onto maps depicting the spatial distribution of the static stress changes due to the 2003 main shock. The static stress changes are calculated, at a depth of 8 km and an apparent coefficient of friction μ=0.6, firstly, for a dextral strike slip fault in agreement with the fault plane solution of the May 1983 event (28°/82°/172°) which is the stronger event located in the vicinity of M4.8's (16/11/2003) epicenter. Figure 5a evidences that the members of this secondary sequence,

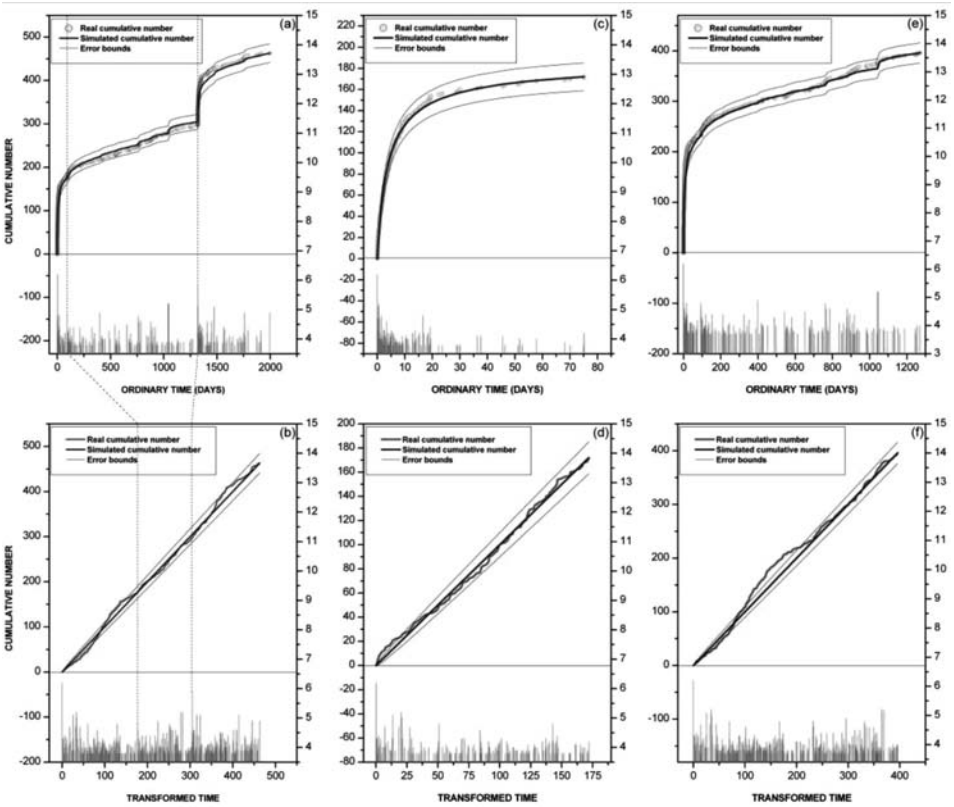

Fig. 4: Cumulative number of earthquakes (yellow circles and red solid lines) against ordinary (a, c, e) and transformed (b, d, f) lapse time respectively, in addition to the theoretically expected cumulative function (blue solid lines) due to the best fitting statistical model. Thin, solid blue lines stand for error bounds. Dashed lines appoint specific time periods and moments during the sequence evolution. (a, b), (c, d), (e, f) correspond to the first, second and third data sets, respectively.

which increased the rate of real seismicity (Fig. 4a) are located inside the southern lobe of positive Coulomb stress changes. The stress field is then calculated according to the fault plane solution of the M5.7 event (216°/75°/–175°). It is observed that this main event and its aftershocks, which comprise the intense seismicity period, are located mainly into the southern lobe of positive stress changes (Fig. 5b).

4. Conclusions

From the temporal distribution of Skyros aftershock sequence, a precursory relative quiescence was observed before the stronger aftershock of M5.4, which occurred in the first day after the main shock. This fact in association with the location of this particular aftershock epicentre into the positive stress changes lobe, guides to the conclusion that assessment of a seismic excitation inside a seismic sequence, in real time, is quite possible. It is remarkable that this period was revealed when the appropriate model was applied at the second data set only, which covered the time interval between the main shock and just before the M5.4 event, but not in the model application to the whole data set.

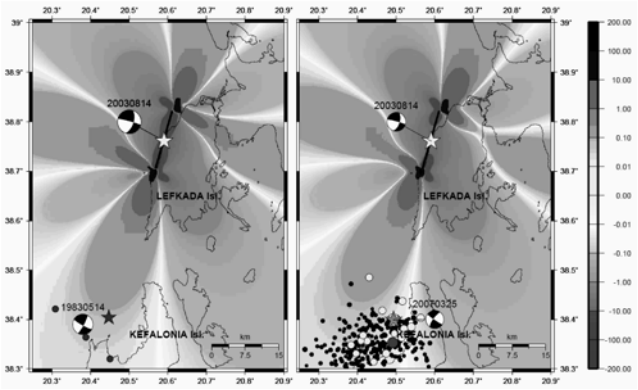

Fig. 5: Static Coulomb stress changes (in bars), due to Lefkada main shock (yellow star) at a depth of 8 km with μ=0.6 (a) for a representative dextral strike slip fault (28°/82°/172°) of an event occurred on May 1983 near to the M4.8 aftershock (blue star). Blue circles show the epicenters of a cluster of aftershocks that followed the M4.8, all located into the southern lobe of positive stress changes. (b) Static stress changes calculated for the M5.7 event (orange star) faulting type (216°/75°/-175°). Aftershocks of magnitudes $2.5 \leq M_w \leq 4.0$ are shown with red circles, $4.0 \leq M_w < 5.0$ with green circles and the ones of $5.0 \leq M_w < 5.7$ with blue circles. M5.7 and its aftershocks are located, mainly, into the southern lobe of positive stress changes.

The analysis of Lefkada seismic sequence evidences abrupt changes in the occurrence rate of aftershocks and later seismicity, after the occurrence of two strong events. The spatial distribution of the members of these two secondary sequences is associated with positive static stress changes, revealing their possible triggering form the 2003 main shock.

Finally, analysis of different sets in both sequences evidenced that the most appropriate statistical model that fits the data can be different, when the analysis concerns different data sets even inside the same aftershock sequence.

5. Acknowledgments

The software 'RETAS statistical model' (Gospodinov and Rotondi, 2006) was used for the statistical analysis, the GMT system (Wessel and Smith, 1998) to plot some of the figures, the program DIS3D (Erikson, 1986 and expressions of G. Converse) for stress changes calculation, the ZMAP software (Wiemer and Zuniga, 2001) for magnitude distribution. This work has been partially supported by project RS09–FF–011/15.04.2009 of Plovdiv University 'Paisii Hilendarski', Bulgaria. Geophysics Department contribution 756.

6. References

Akaike, H., 1974. A new look at the statistical model identification, IEEE Trans. Automat. Control., AC–19, 716–723.

Erikson, L., 1986. User's manual for DIS3D: A three-dimensional dislocation program with applications to faulting in the Earth. Masters Thesis, Stanford Univ., Stanford, Calif., 167pp.

Ganas, A., Drakatos, G., Pavlides, S. B, Stavrakakis, G. N, Ziazia, M., Sokos, E., and Karastathis, V. K., 2005. The 2001 M_w=6.4 Skyros earthquake, conjugate strike–slip faulting and spatial variation in stress within the central Aegean Sea. J. Geodynamics, 39, 61–77.

Gospodinov, D. and Rotondi, R., 2006. Statistical analysis of triggered seismicity in Kresna region of SW Bulgaria, (1904) and the Umbria–Marche Region of Central Italy (1997). Pure Appl. Geophys, 163, 1597–1615.

Karakostas, V. G., Papadimitriou, E. E. and Papazachos, C. B., 2004. Properties of the 2003 Lefkada, Ionian Islands, Greece, earthquake seismic sequence and seismicity triggering, Bull. Seism. Soc. Am., 87, 463–473.

Karakostas, V. G., 2008. Relocation of aftershocks of the 2003 Lefkada sequence: Seismotectonic implications /Proc. 3rd Hellenic Conf. Earthquake Engineering & Engineering Seismology, Athens 5–7 Nov. 2008/, CD ROM, pp.16.

Kisslinger, C., 1988. An experiment in earthquake prediction and the 7th May 1986 Andreanof Islands earthquake, Bull. Earthquake Res. Inst. Univ. Tokyo, 61, 1–65.

Ogata, Y., 1988. Statistical models for earthquake occurrences and residual analysis for point processes. J. Am. Stat. Assoc. 83, 9–27.

Ogata, Y., 1992. Detection of precursory relative quiescence before great earthquakes through a statistical model, J. Geophys. Res., 97, 19, 845-19,871.

Ogata, Y., 1999. Seismicity analyses through point process modeling: A review, Pure Appl. Geophys., 155, 471–507.

Ohtake, M., T. Matumoto, and G. V. Latham, 1997. Seismicity gap near Oaxaca, southern Mexico as a probable precursor to a large earthquake, Pure Appl. Geophys., 115, 375–385.

Omori, F., 1894.On the aftershocks of earthquakes. J.Coll. Sci., Imp. Univ. Tokyo 7, 111-200.

Papazachos, B. C., E. E. Papadimitriou, A. A. Kiratzi, C. B. Papazachos, and E. K. Louvari, 1998. Fault plane solutions in the Aegean and the surrounding area and their tectonic implications, Bull. Geof. Teor. Appl., 39, 199–218.

Papazachos, B. C. and P. E. Comninakis, 1971. Geophysical and tectonic features of the Aegean Arc, J. Geophys. Res. 76, 8517–8533.

Roumelioti, Z., Kiratzi, A. and Dreger, D., 2004. The source process of the 2001 July 26 Skyros Island (Greece) earthquake, Geophys. J. Intern., 156, 541–548.

Scordilis, E. M., Karakaisis, G. F., Karakostas, B. G., Panagiotopoulos, D. G., Comninakis, P. E. and Papazachos, B. C., 1985. Evidence for transform faulting in the Ionian Sea: The Cephalonia Island earthquake sequence, Pure Appl. Geophys., 123, 288–397.

Utsu, T., 1968. Seismic activity in Hokkaido and its vicinity (in Japanese), Geophys. Bull. Hokkaido Univ., 13, 99–103.

Utsu, T., 1969. Aftershocks and earthquake statistics (I): some parameters which characterize an aftershock sequence and their interaction. J. Fac. Sci., Hokkaido Univ., Ser. VII 3, 129–195.

Wessel, P. and Smith, W. H. F., 1998. New, improved version of the Generic Mapping tools Released, EOS Trans. AGU, 79, 579.

Wiemer, S. and Zuniga, R. F., 2001. ZMAP: A software package to analyze seismicity, EOS, Trans, 44, 456.

Wyss, M., and R. O. Burford, 1987. A predicted earthquake on the San Andreas fault, California, Nature, 329, 323–325.

Zahradnik, J., 2002. The weak–motion modelling of the Skyros island, Aegean Sea M_w=6.5 earthquake of July 26. Studia Geophys. Geodaet., 46, 753–771.